Published in Applied Physics Letters. Please cite: J. F. Ihlefeld, T. Peters, S. T. Jaszewski, T. Mimura, B. L. Aronson and S. Trolier-McKinstry, "Applied in-plane strain effects on the polarization response of ferroelectric hafnium zirconium oxide thin films," *Applied Physics Letters* **123** (8) (2023). https://doi.org/10.1063/5.0165072

Applied In-Plane Strain Effects on the Polarization Response of Ferroelectric Hafnium Zirconium Oxide Thin Films

Jon F. Ihlefeld,[1, 2, a)] Travis Peters,[3] Samantha T. Jaszewski,[1] Takanori Mimura,[1, b)] Benjamin L. Aronson,[1] and Susan Trolier-McKinstry[3, a)]

[1]Department of Materials Science and Engineering, University of Virginia, Charlottesville, VA 22904, USA

[2]Charles L. Brown Department of Electrical and Computer Engineering, University of Virginia, Charlottesville, VA, 22904, USA

[3]Materials Science and Engineering Department and Materials Research Institute, The Pennsylvania State University, University Park, PA 16802, USA

The influence of biaxial stress on the maximum and remanent polarizations of 10 nm thick hafnium zirconium oxide thin films in metal-ferroelectric-metal capacitor structures has been quantified. In the as-prepared state with a nominal biaxial tensile strain of 0.20% and no applied extrinsic stress, remanent and maximum polarizations of 7.6 and 13.1 μC/cm^2, respectively, were measured using a 2 MV/cm applied electric field. Reducing the intrinsic strain by 0.111% through the application of a compressive uniaxial stress results in a decrease of the remanent and maximum polarizations to 6.8 and 12.2 μC/cm^2, respectively. The polarization dependence on strain is nearly linear between these values. The observed variation in polarization with strain is consistent with strain impacting ferroelastic switching whereby in-plane tension increases the fraction of the short polar axis orienting out-of-plane, hence increasing out-of-plane polarization. In contrast, reducing the in-plane strain through compression results in an increase in the fraction of the long non-polar axis orienting out-of-plane, thereby decreasing out-of-plane polarization.

[a)] Authors to whom correspondence should be addressed: jihlefeld@virginia.edu, set1@psu.edu
[b)] Present Address: Gakushuin University

Ferroelectricity in hafnium oxide has attracted significant attention since its first report in 2011[1] owing to its inherent thermodynamic compatibility with mainstream semiconductors,[2] ability to maintain large switchable polarizations to sub-10 nm thicknesses without requiring epitaxy,[3] and large-scale semiconductor fabrication compatibility. These attributes have made it attractive for many microelectronic memory applications, with promise toward achieving non-volatile memory in back-end-of-line (BEOL) layers of an integrated circuit in ferroelectric random access memory (FeRAM), ferroelectric tunnel junctions (FTJs), or ferroelectric field effect transistors (FeFETs).

The observation of ferroelectricity in a fluorite-structured oxide was initially unexpected, and the ferroelectric response has been attributed to a non-centrosymmetric, metastable orthorhombic phase with space group $Pca2_1$.[1, 4] There are several factors that are known to influence phase stability and ferroelectric performance in hafnia. These include substituents or alloying with elements such as zirconium;[5] oxygen vacancies;[6-8] sub-micron crystalline dimensions;[9, 10] capping electrode layers;[1, 10-14] and in-plane tensile stress.[14-19] Mechanical stress, in particular, has been shown to be important to the ferroelectric response. There are two mechanisms for this: 1) tensile stress aids in stabilizing the ferroelectric phase, and 2) in-plane tensile stress aids in orienting the polar *c*-axis out of the plane of the film, resulting in a larger switchable polarization. The former has recently been computationally demonstrated by Zhou *et al.*, where tensile stress has been shown to stabilize an antipolar mode in the metastable tetragonal phase, which concomitantly stabilizes a polar mode and leads to the transformation to and stabilization of the $Pca2_1$ phase.[20] The latter has been demonstrated both with synchrotron X-ray diffraction and scanning transmission Kikuchi diffraction characterization where the short non-ferroelectric *b*-axis was identified as being out-of-plane in pristine devices and an increasing fraction of intermediate length polar *c*-axis was found to be out-of-plane in awoken devices, suggesting that ferroelastic switching is part of the wake-up process.[21, 22] In addition, multiple research groups have shown a direct correlation of tensile stress with remanent polarization magnitude.[14, 15, 18, 23]

The majority of experiments conducted to isolate stress effects on the ferroelectric response in hafnia have been performed under static, *ex-situ* conditions. That is, the films are prepared with some stress state that is quantified, and the ferroelectric properties are measured. There are few reports of the effect of an intentionally applied stress on the ferroelectric response of hafnia. In one example, Kruv *et al*. showed that electric field cycling under an applied in-plane compressive stress led to larger magnitudes of switchable polarization increase associated with wake-up than when cycling was conducted under an in-plane tensile stress.[24] It was postulated that in-plane compressive stress preferentially promoted polarization orientation in the measurement direction with the applied field. Liu *et al*. studied the effects of strain on the polarization response of hafnium zirconium oxide films prepared on mica substrates and observed essentially no variability with compressive or tensile stresses as the film/substrate stacks were

wrapped around mandrels of differing radii.[25] However, it should be noted that the weak interlayer bonding in mica substrates and the potential thin substrate thicknesses may have resulted in limited strain transfer to the hafnia layers. Additionally, Zhong *et al*. transferred epitaxially-grown HZO membranes to mica substrates and observed no change in remanent polarization as the film/substrate stack was bent to provide a 0.05% tensile strain at the surface of the mica substrate.[26] In this case, the strong 111 out-of-plane orientation of the epitaxially-grown film should not exhibit ferroelastic differences to polarization under different strain states because of degeneracy of the 111 *d*-spacing, and the same issue of stress transfer in mica substrates discussed previously exists. Finally, Yu *et al*. observed an increase in the remanent polarization under in-plane tensile strain for hafnium zirconium oxide films prepared on polyimide substrates and bent to different radii of curvature; however, the strain magnitude was not reported.[27]

In the present work, the effect of applied mechanical stress on the maximum measured and remanent polarizations of 10 nm thick hafnium zirconium oxide (HZO) films on silicon substrates was assessed, and the stress and strains were quantified. It is shown that the intrinsic in-plane tensile stress that is present from processing results in the largest realizable maximum and remanent polarizations, while the application of a compressive stress decreases the maximum and remanent polarizations. The results are consistent with tensile stress aiding the orientation of the polar axis out of the plane of the film via a ferroelastic response.

Stacked structures of 100 nm Pt/20 nm TaN/10 nm HZO/100 nm TaN/Si were prepared following procedures published previously.[28] Briefly, TaN bottom and top contacts were prepared by DC magnetron sputtering from a sintered TaN target. Hafnium zirconium oxide thin films were prepared via plasma-enhanced atomic layer deposition (PE-ALD) within an Oxford FlexAL II instrument using tetrakis(ethylmethylamido)hafnium and tetrakis(ethylmethylamido)zirconium as metal precursors and an oxygen plasma as the oxygen source. A dose ratio of 6:4 Hf:Zr was used with 8 supercycles to achieve the desired thickness with a platen temperature of 260 °C. The 6:4 ratio was shown in prior work to result in an approximate $Hf_{0.5}Zr_{0.5}O_2$ composition. After deposition of the top TaN layer, the structure was rapid thermal annealed at 700 °C for 30 seconds in 1 atmosphere of flowing (5 slm) N_2 gas within an Allwin21 AccuThermo AW 610 instrument. Photolithography was used to pattern top electrode contacts and was followed by evaporation of platinum, liftoff, and submersion in an SC-1 bath to define the capacitor structures and etch TaN from the field. The wafer was cleaved into an approximately 5 cm × 1 cm cantilever beam, and a strain gage (Omega Engineering, gauge factor=1.95 ± 1.5 %) was affixed to the surface of the structure using a cyanoacrolyte adhesive approximately 1 cm from the end of the sample. The same end of the cantilever was clamped, and the opposing end was positioned over a multilayer piezoelectric actuator (Kinetic Ceramics), which was used to deflect the cantilever to be concave toward

the film side (i.e., the film side was uniaxially compressed in-plane). A schematic of the device structure and mechanical strain apparatus is shown in Supplemental Materials, Figure S1; additional details on the fixture are described in Coleman *et al*.[29]

Field cycling for wake-up was performed using a 2 MV/cm triangular wave applied at 10 kHz and was conducted prior to measuring capacitors under differing stress states. Polarization versus electric field ($P(E)$) hysteresis was performed on 200 μm diameter capacitors using a Radiant Technologies Precision Multiferroic instrument with a measurement period of 0.1 ms and a maximum field of 2 MV/cm. Stable polarization hysteresis response was measured after 2500 cycles (Supplemental Materials, Figure S2). The $P(E)$ response on an awoken capacitor (i.e. after application of 3500 2 MV/cm cycles) during the application of compressive stress was measured three times for each stress state, and the remanent and maximum-measured polarizations were averaged. Grazing-incidence X-ray diffraction (XRD) was performed to identify the phases present using a Malvern Panalytical Empyrean instrument using Cu-Kα radiation with an incidence angle of 0.7°, a parallel plate collimator on the diffracted beam optics, and a proportional counter point detector. Phase constitution was determined by fitting the diffraction peaks with LIPRAS software[30] and pseudo-Voigt peak shapes. The initial strain state of an HZO capacitor was measured using the $\sin^2\psi$ XRD technique with a Bruker D8 Venture instrument equipped with an Incoatec IμS 3.0 Cu-Kα collimated source and a Photon III 2-dimensional detector in a reflection geometry with an incidence angle of 15°. A magnesium oxide powder was applied to the film surface to serve as a standard and enable accurate *d*-spacing extraction by pyFAI software.[31] The calculation of strain and stress utilized procedures and biaxial moduli values published previously.[28] In the $\sin^2\psi$ measurement of strain and calculation of stress, an assumption of homogeneous stress in the film is assumed. This is a reasonable assumption for a very thin film prepared atop a thick high-modulus substrate with lateral dimensions well in excess of the substrate thickness.

Figure 1(a) shows the grazing-incidence XRD pattern of the film and the fit to the metastable orthorhombic (*o*) and/or tetragonal (*t*) phases. It was found that the film contained no monoclinic (*m*) phase within the detection limits of the XRD experiment, and this is true even as the grazing-incidence XRD geometry samples areas of the film where the top electrode had been removed. This is known to result in some fraction of the film transforming into the monoclinic phase by removing the local membrane force applied by the top electrode.[13]

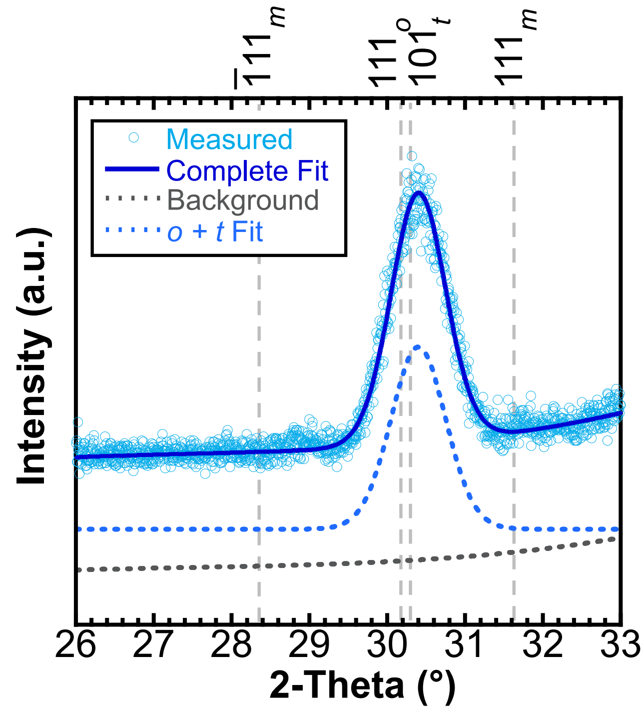

FIG. 1. Grazing incidence X-ray diffraction pattern of the 10 nm thick $Hf_{0.5}Zr_{0.5}O_2$ thin film and fit to illustrate the absence of the monoclinic phase.

The unwrapped 2D diffraction pattern for the capacitor stack is shown in Figure 2(a). No evidence of a monoclinic phase is observed, and no crystallographic texture is seen for the HZO phases. The TaN and platinum films both exhibit out-of-plane texture, as indicated by the intense diffraction signals for values near 0° in ψ. Using d-spacing of the $111_o/011_t$ diffraction peak as a function of ψ angle, the biaxial stress of the HZO layer was calculated to be 0.78 ± 0.2 GPa tensile, which corresponds to a biaxial strain of 0.20%, as shown in Figure 2(b).

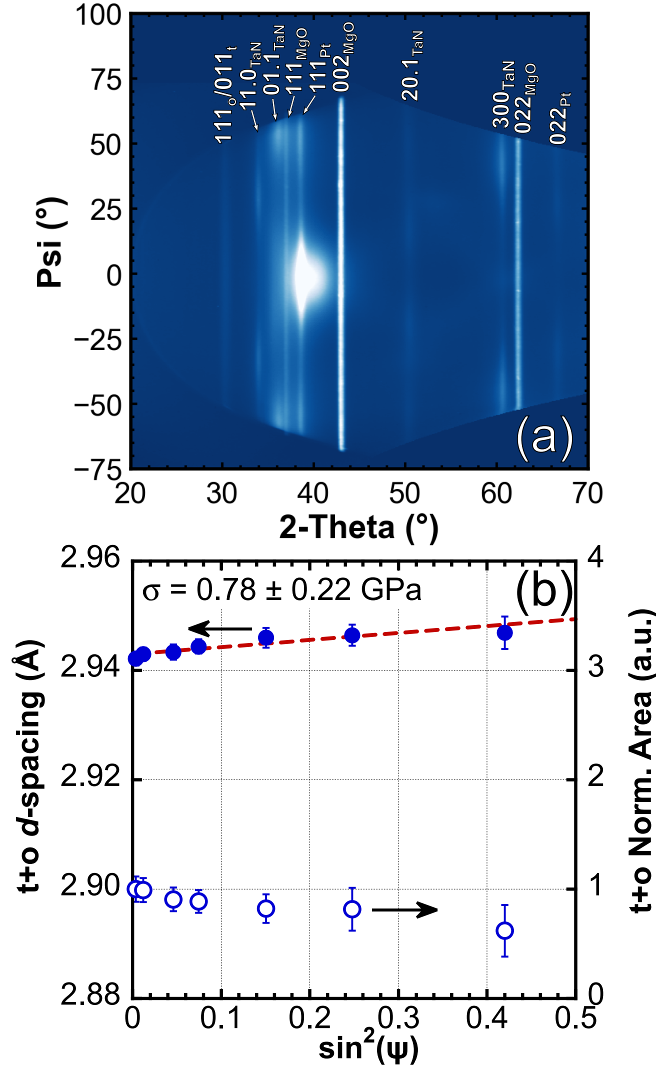

FIG. 2. (a) 2-dimensional diffraction pattern collected on an individual Pt/TaN/HZO/TaN/Si capacitor. (b) *d*-spacing of the *t*+*o* (tetragonal and orthorhombic phases) diffraction peak as a function of the $\sin^2\psi$ value and the associated fit (red dashed line). The right axis is the normalized intensity of the *t*+*o* peak with $\sin^2\psi$ angle.

Strain measured by the strain gauge adhered to the sample was used to determine the strain and stress in the HZO film as a function of the applied load. The measured strains were used to calculate the change in stress in the HZO layer through the use of the HZO biaxial modulus (294 GPa).[28] It was assumed that the initial strain in the HZO capacitor was 0.20% tensile, as determined by the $\sin^2\psi$ measurement. A compressive stress was applied to the cantilever by the piezoelectric actuator and resulted in a maximum change in strain of -0.111%. This maximum applied compressive strain of -0.111% corresponds to a stress decrease in the HZO of 320 MPa to an estimated value of 460

± 200 MPa, or a stress decrease of approximately 40%. The cantilever fractured after the -0.111% strain measurement. To simplify the discussion below, extrinsic strains will be reported, which refer to the strain applied to the film and does not account for the 0.20% intrinsic biaxial tensile strain present in the HZO capacitor due to processing (i.e., due to densification of the HZO film, thermal expansion coefficient mismatch with the substrate, and the membrane force from the top electrode preventing the formation of the monoclinic phase[13]).

Electric field-driven polarization hysteresis measured during the application of stress to the device is shown in Figure 3(a), where the extrinsic strain in the HZO layer is reported. The three individual measurements for each strain state are provided in Supplemental Materials, Figure S3. For each strain, well-saturated polarization hysteresis is observed with no obvious signatures of leakage current artifacts. The coercive fields are relatively invariant with applied stress and are approximately -0.8 and 1.2 MV/cm, though it is noted that there is a slight decrease in the negative coercive field with increasing applied compressive strain. The observed imprint of 0.2 MV/cm corresponds with a 0.2 V potential difference between the top and bottom electrodes. This is likely due to the difference in the energy barriers for the two electrodes owing to the bottom electrode being exposed to the PE-ALD processing conditions while the top electrode was not.[32] This is further supported by the observation that metals of different work functions can drive imprint in thin hafnia-based capacitors.[33] The magnitude of the maximum and remanent polarizations do vary with stress, as shown in Figure 3(b). The initial condition of no applied stress and no extrinsic strain results in the largest maximum and remanent polarizations of 13.1 ± 0.01 and 7.63 ± 0.01 $\mu C/cm^2$, respectively. While no stress had been applied, the HZO film was in a state of tensile in-plane strain. Conversely, uniaxially compressively straining the film resulted in a reduction of both maximum and remanent polarizations to 12.2 ± 0.004 and 6.83 ± 0.01 $\mu C/cm^2$, respectively, for a strain of -0.111%. For intermediate extrinsic strains, the polarization values scale nearly linearly.

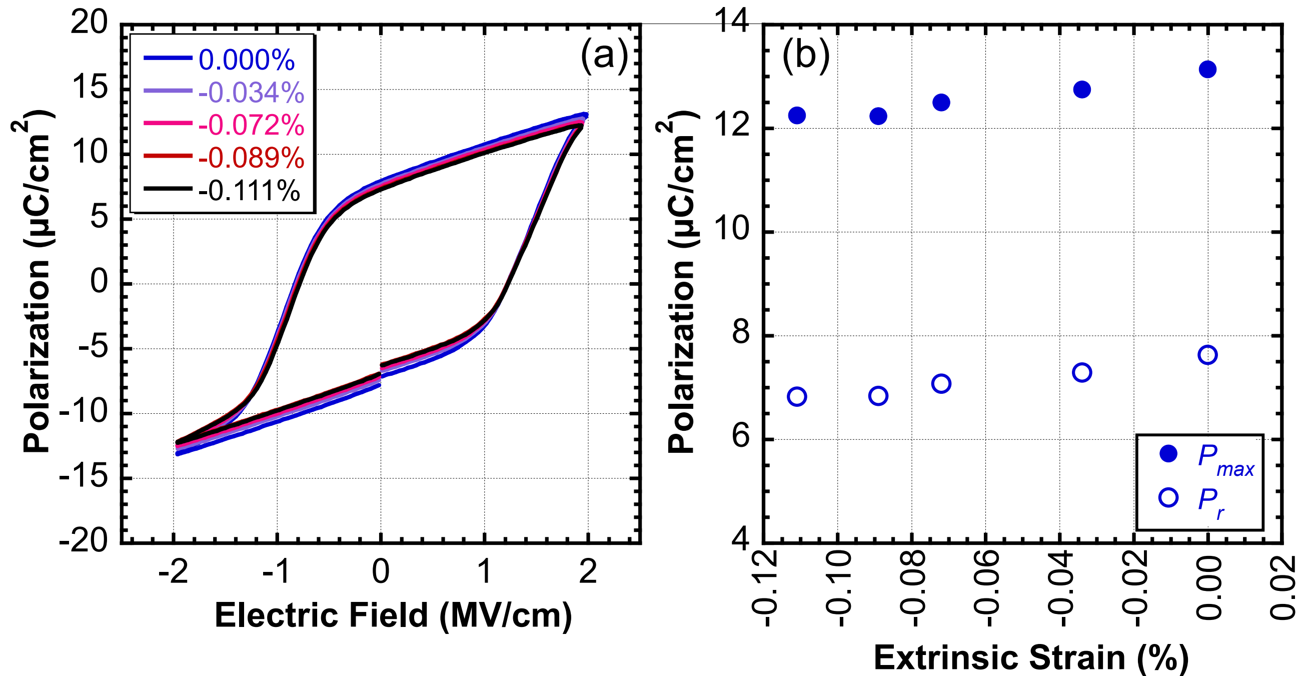

FIG. 3. (a) *P*(*E*) response of Pt/TaN/HZO/TaN/Si capacitors with varying degrees of applied strain. (b) Maximum polarization (P_{max}, closed data points) measured at 2 MV/cm, and remanent polarization (P_r, open data points) for HZO with varying applied strain levels. Error bars on data are smaller than data points.

These results, which show a maximum polarization with no extrinsic strain and a decreasing polarization with in-plane compressive strain, are consistent with a ferroelastic origin of the strain-polarization dependence. The lattice parameters of the $Pca2_1$ hafnia phase are a = 5.24, b = 5.06, and c = 5.07 Å,[4] and the polar axis is the *c*-axis. As such, large in-plane tensile strains would be expected to favor the *a*-axis in-plane and the *b*- and *c*-axes out-of-plane. Given the small differences between the lengths of *b*- and *c*-axes, it is reasonable to assume that the application of an electric field along with strain will favor alignment of the *c*-axis out-of-plane, giving rise to larger remanent and maximum polarizations. A compressive strain, however, would favor orienting the long *a*-axis out-of-plane, which decreases remanent and maximum polarizations. This model is consistent with prior observations of the progression of polarization magnitude with poling and wake-up field cycling.[21, 22] There remains a possibility that a compressive stress (or a reduction of the tensile stress) could favor formation of the tetragonal phase, which has been reported to have a smaller molar volume than the ferroelectric orthorhombic phase.[34] If the reduction in stress was leading to a phase transformation to the tetragonal phase, it would be anticipated that pinching of the *P*(*E*) response would be observed as the tetragonal phase typically behaves as a field-induced ferroelectric, which exhibits antiferroelectric-like polarization

behavior. Additionally, an increase in the slope of the $P(E)$ response at saturating fields would be expected[35] as the relative permittivity of the tetragonal phase is reportedly larger than the ferroelectric orthorhombic phase.[36] That neither of these behaviors were observed, suggests that the ferroelastic mechanism is dominant here. Further, it should be noted that the strains measured and stresses applied in this work are relatively small compared to the stresses possible in hafnia-based films, where values of several GPa have been reported.[14, 18, 28] For the 320 MPa change in stress reported in this study, the maximum and remanent polarizations each varied by approximately 1 $\mu C/cm^2$. Extrapolating to a stress of 4 GPa indicates an increase in remanent polarization by 10 $\mu C/cm^2$, which is consistent with measured remanent polarizations for HZO films of similar composition and stress level.[14] This suggests that the large remanent polarizations that are typically observed in hafnia-based capacitors (e.g., > 20 $\mu C/cm^2$) are, at least in part, due to ferroelastic orienting of the polar *c*-axis out-of-plane.

In summary, this work illustrates the polarization sensitivity of HZO capacitors to applied stress. It was found that the measured maximum and remanent polarizations varied by approximately 1 $\mu C/cm^2$ over an applied in-plane stress of 320 MPa, which corresponds with a strain variation of 0.111%. These results are consistent with an increase in ferroelastic switching for in-plane tensile stresses that favor orienting the short polar *c*-axis out-of-plane of the film. This illustrates that hafnia-based thin film devices are sensitive to applied stresses and that stress can be used to tailor polarization magnitude in this material system.

SUPPLEMENTARY MATERIAL

See the supplementary material for a schematic of the stress-application fixture, polarization hysteresis during wake-up field cycling, and polarization hysteresis measured for each stress application.

ACKNOWLEDGEMENTS

This material is based upon work supported by the Center for 3D Ferroelectric Microelectronics (3DFeM), an Energy Frontier Research Center funded by the U.S. Department of Energy, Office of Science, Office of Basic Energy Sciences Energy Frontier Research Centers program under Award Number DE-SC0021118. S.T.J. acknowledges support from a U.S. National Science Foundation Graduate Research Fellowship under Award DGE-1842490. This work utilized a Bruker D8 Venture instrument, which was acquired under Award CHE-2018870 from the U.S. National Science Foundation's Major Research Instrumentation program.

AUTHOR DECLARATIONS

Conflict of Interest

The authors have no conflicts to disclose.

Author Contributions

Jon F. Ihlefeld: conceptualization (equal); writing – original draft (lead); investigation (equal); funding acquisition (equal). Travis Peters: investigation (equal); writing – original draft (supporting). Samantha T. Jaszewski: investigation (equal); writing – original draft (supporting); funding acquisition (supporting). Takanori Mimura: investigation (equal); writing – original draft (supporting). Benjamin L. Aronson: investigation (supporting). Susan Trolier-McKinstry: conceptualization (equal); investigation (equal), writing – original draft (supporting); funding acquisition (lead).

DATA AVAILABILITY

The data that support the findings of this study are available from the corresponding author upon reasonable request.

References

1. T. S. Böscke, J. Möller, D. Bräuhaus, U. Schröder and U. Böttger, Appl. Phys. Lett. **99** (10), 102903 (2011).

2. K. J. Hubbard and D. G. Schlom, J. Mater. Res. **11** (11), 2757-2776 (1996).

3. S. S. Cheema, D. Kwon, N. Shanker, R. dos Reis, S.-L. Hsu, J. Xiao, H. Zhang, R. Wagner, A. Datar, M. R. McCarter, C. R. Serrao, A. K. Yadav, G. Karbasian, C.-H. Hsu, A. J. Tan, L.-C. Wang, V. Thakare, X. Zhang, A. Mehta, E. Karapetrova, R. V. Chopdekar, P. Shafer, E. Arenholz, C. Hu, R. Proksch, R. Ramesh, J. Ciston and S. Salahuddin, Nature **580** (7804), 478-482 (2020).

4. X. Sang, E. D. Grimley, T. Schenk, U. Schroeder and J. M. LeBeau, Appl. Phys. Lett. **106** (16), 162905 (2015).

5. J. Müller, T. S. Böscke, U. Schröder, S. Mueller, D. Bräuhaus, U. Böttger, L. Frey and T. Mikolajick, Nano Lett. **12** (8), 4318-4323 (2012).

6. A. Pal, V. K. Narasimhan, S. Weeks, K. Littau, D. Pramanik and T. Chiang, Appl. Phys. Lett. **110** (2), 022903 (2017).

7. T. Mittmann, M. Materano, S. C. Chang, I. Karpov, T. Mikolajick and U. Schroeder, presented at the 2020 IEEE International Electron Devices Meeting (IEDM), 2020 10.1109/iedm13553.2020.9372097.

8. S. T. Jaszewski, E. R. Hoglund, A. Costine, M. H. Weber, S. S. Fields, M. G. Sales, J. Vaidya, L. Bellcase, K. Loughlin, A. Salanova, D. A. Dickie, S. L. Wolfley, M. D. Henry, J.-P. Maria, J. L. Jones, N.

Shukla, S. J. McDonnell, P. Reinke, P. E. Hopkins, J. M. Howe and J. F. Ihlefeld, Acta Mater. **239**, 118220 (2022).

9. R. Materlik, C. Künneth and A. Kersch, J. Appl. Phys. **117** (13), 134109 (2015).
10. M. H. Park, Y. H. Lee, H. J. Kim, T. Schenk, W. Lee, K. D. Kim, F. P. G. Fengler, T. Mikolajick, U. Schroeder and C. S. Hwang, Nanoscale **9** (28), 9973-9986 (2017).
11. P. Polakowski and J. Müller, Appl. Phys. Lett. **106** (23), 232905 (2015).
12. T. Nishimura, L. Xu, S. Shibayama, T. Yajima, S. Migita and A. Toriumi, Jpn. J. Appl. Phys. **55** (8S2), 08pb01 (2016).
13. S. S. Fields, T. Cai, S. T. Jaszewski, A. Salanova, T. Mimura, H. H. Heinrich, M. D. Henry, K. P. Kelley, B. W. Sheldon and J. F. Ihlefeld, Adv. Electron. Mater. **8** (12), 2200601 (2022).
14. J. F. Ihlefeld, S. T. Jaszewski and S. S. Fields, Appl. Phys. Lett. **121** (24), 240502 (2022).
15. T. Shiraishi, K. Katayama, T. Yokouchi, T. Shimizu, T. Oikawa, O. Sakata, H. Uchida, Y. Imai, T. Kiguchi, T. J. Konno and H. Funakubo, Appl. Phys. Lett. **108** (26), 262904 (2016).
16. T. Shiraishi, K. Katayama, T. Yokouchi, T. Shimizu, T. Oikawa, O. Sakata, H. Uchida, Y. Imai, T. Kiguchi, T. J. Konno and H. Funakubo, Mat. Sci. Semicon. Proc. **70**, 239-245 (2017).
17. S. J. Kim, D. Narayan, J.-G. Lee, J. Mohan, J. S. Lee, J. Lee, H. S. Kim, Y.-C. Byun, A. T. Lucero, C. D. Young, S. R. Summerfelt, T. San, L. Colombo and J. Kim, Appl. Phys. Lett. **111** (24), 242901 (2017).
18. T. Schenk, C. M. Fancher, M. H. Park, C. Richter, C. Künneth, A. Kersch, J. L. Jones, T. Mikolajick and U. Schroeder, Adv. Electron. Mater. **5** (12), 1900303 (2019).
19. S. Estandía, N. Dix, J. Gazquez, I. Fina, J. Lyu, M. F. Chisholm, J. Fontcuberta and F. Sánchez, ACS Appl. Electron. Mater. **1** (8), 1449-1457 (2019).
20. S. Zhou, J. Zhang and A. M. Rappe, Sci. Adv. **8** (47), eadd5953 (2022).
21. M. Lederer, R. Olivo, D. Lehninger, S. Abdulazhanov, T. Kämpfe, S. Kirbach, C. Mart, K. Seidel and L. M. Eng, Phys. Status Solid-R. **15** (5), 2100086 (2021).
22. T. Shimizu, T. Mimura, T. Kiguchi, T. Shiraishi, T. Konno, Y. Katsuya, O. Sakata and H. Funakubo, Appl. Phys. Lett. **113** (21), 212901 (2018).
23. M. Lederer, T. Kämpfe, R. Olivo, D. Lehninger, C. Mart, S. Kirbach, T. Ali, P. Polakowski, L. Roy and K. Seidel, Appl. Phys. Lett. **115** (22), 222902 (2019).
24. A. Kruv, S. R. C. McMitchell, S. Clima, O. O. Okudur, N. Ronchi, G. Van den bosch, M. Gonzalez, I. De Wolf and J. V. Houdt, in *2021 IEEE International Reliability Physics Symposium (IRPS)* (2021), pp. 1-6.
25. W.-Y. Liu, J.-J. Liao, J. Jiang, Y.-C. Zhou, Q. Chen, S.-T. Mo, Q. Yang, Q.-X. Peng and L.-M. Jiang, J. Mater. Chem. C **8** (11), 3878-3886 (2020).

26. H. Zhong, M. Li, Q. Zhang, L. Yang, R. He, F. Liu, Z. Liu, G. Li, Q. Sun, D. Xie, F. Meng, Q. Li, M. He, E. J. Guo, C. Wang, Z. Zhong, X. Wang, L. Gu, G. Yang, K. Jin, P. Gao and C. Ge, Adv. Mater. **34** (24), 2109889 (2022).

27. H. Yu, C.-C. Chung, N. Shewmon, S. Ho, J. H. Carpenter, R. Larrabee, T. Sun, J. L. Jones, H. Ade, B. T. O'Connor and F. So, Adv. Funct. Mater. **27** (21), 1700461 (2017).

28. S. S. Fields, D. H. Olson, S. T. Jaszewski, C. M. Fancher, S. W. Smith, D. A. Dickie, G. Esteves, M. D. Henry, P. S. Davids, P. E. Hopkins and J. F. Ihlefeld, Appl. Phys. Lett. **118** (10), 102901 (2021).

29. K. Coleman, J. Walker, T. Beechem and S. Trolier-McKinstry, J. Appl. Phys. **126** (3), 034101 (2019).

30. G. Esteves, K. Ramos, C. M. Fancher and J. L. Jones, LIPRAS: Line Profile Analysis Software, DOI: 10.13140/RG13142.13142.29970.25282/13143 (2017).

31. G. Ashiotis, A. Deschildre, Z. Nawaz, J. P. Wright, D. Karkoulis, F. E. Picca and J. Kieffer, J. Appl. Crystallogr. **48** (2), 510-519 (2015).

32. M. A. Jenkins, K. E. K. Holden, S. W. Smith, M. T. Brumbach, M. D. Henry, C. Weiland, J. C. Woicik, S. T. Jaszewski, J. F. Ihlefeld and J. F. Conley, Jr., ACS Appl. Mater. Inter. **13** (12), 14634-14643 (2021).

33. S. S. Fields, S. T. Jaszewski, M. K. Lenox and J. F. Ihlefeld, Adv. Mater. Interfaces **10** (8), 2202232 (2023).

34. S. E. Reyes-Lillo, K. F. Garrity and K. M. Rabe, Phys. Rev. B **90** (14), 140103 (2014).

35. M. H. Park, H. J. Kim, Y. J. Kim, Y. H. Lee, T. Moon, K. D. Kim, S. D. Hyun, F. Fengler, U. Schroeder and C. S. Hwang, ACS Appl. Mater. Inter. **8** (24), 15466-15475 (2016).

36. M. H. Park, H. J. Kim, Y. J. Kim, W. Lee, T. Moon and C. S. Hwang, Appl. Phys. Lett. **102** (24), 242905 (2013).

Published in Applied Physics Letters. Please cite: DOI: 10.1063/5.0165072

Supplementary Material for:

Applied In-Plane Strain Effects on the Polarization Response of Ferroelectric Hafnium Zirconium Oxide Thin Films

Jon F. Ihlefeld,[1, 2, a)] Travis Peters,[3] Samantha T. Jaszewski,[1] Takanori Mimura,[1, b)] Benjamin L. Aronson,[1] and Susan Trolier-McKinstry[3, c)]

[1]Department of Materials Science and Engineering, University of Virginia, Charlottesville, VA 22904
[2]Charles L. Brown Department of Electrical and Computer Engineering, University of Virginia, Charlottesville, VA, 22904
[3]Materials Science and Engineering Department and Materials Research Institute, The Pennsylvania State University, University Park, PA 16802

[a)] Electronic Mail: jihlefeld@virginia.edu
[b)] Present Address: Gakushuin University
[c)] Electronic Mail: set1@psu.edu

Published in Applied Physics Letters. Please cite: DOI: 10.1063/5.0165072

FIG. S1.

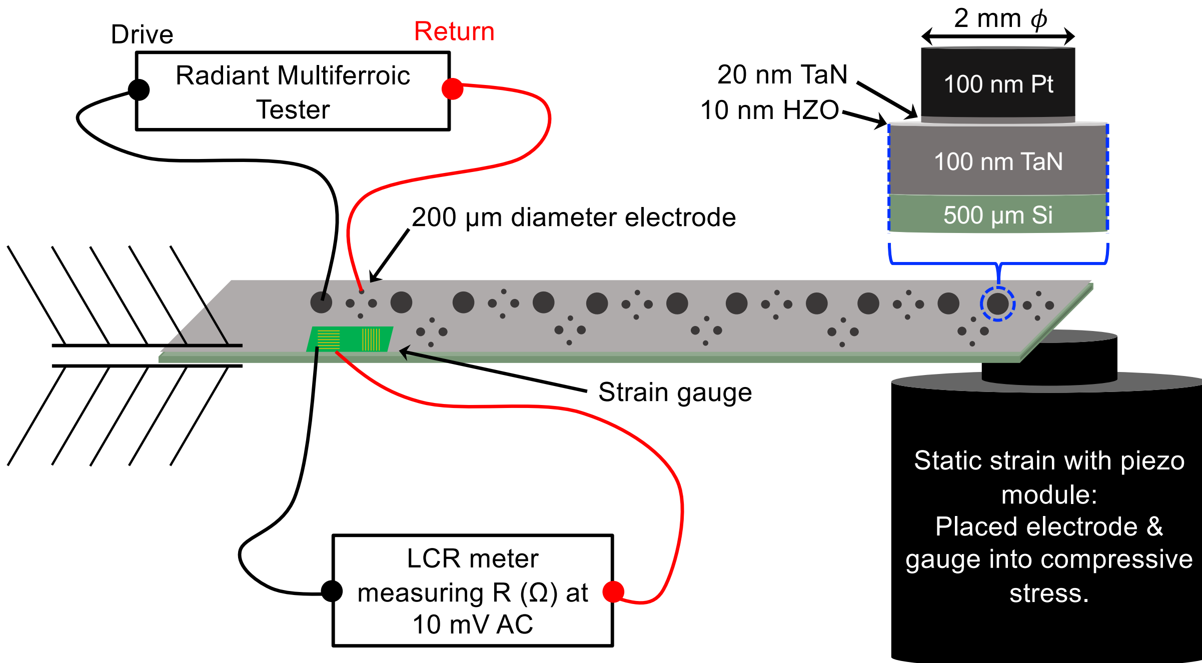

FIG. S1. Schematic of the sample and method by which stress was applied and strain measured in this study. The large "Drive" electrode was electrically shorted to the bottom electrode.

Published in Applied Physics Letters. Please cite: DOI: 10.1063/5.0165072

FIG. S2.

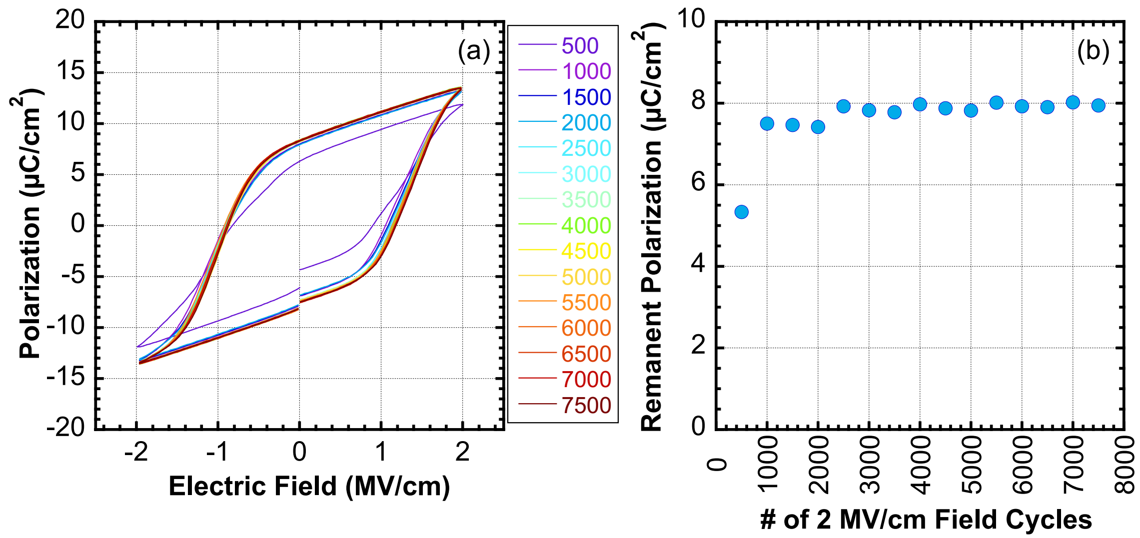

FIG. S2. (a) Polarization versus electric field as a function of the number of 2 MV/cm triangle waves applied at 10 kHz performed and measured without an extrinsically applied stress. (b) Remanent polarization calculated from the *P*(*E*) response shown in (a) as a function of the number of 2 MV/cm triangle waves.

FIG. S3.

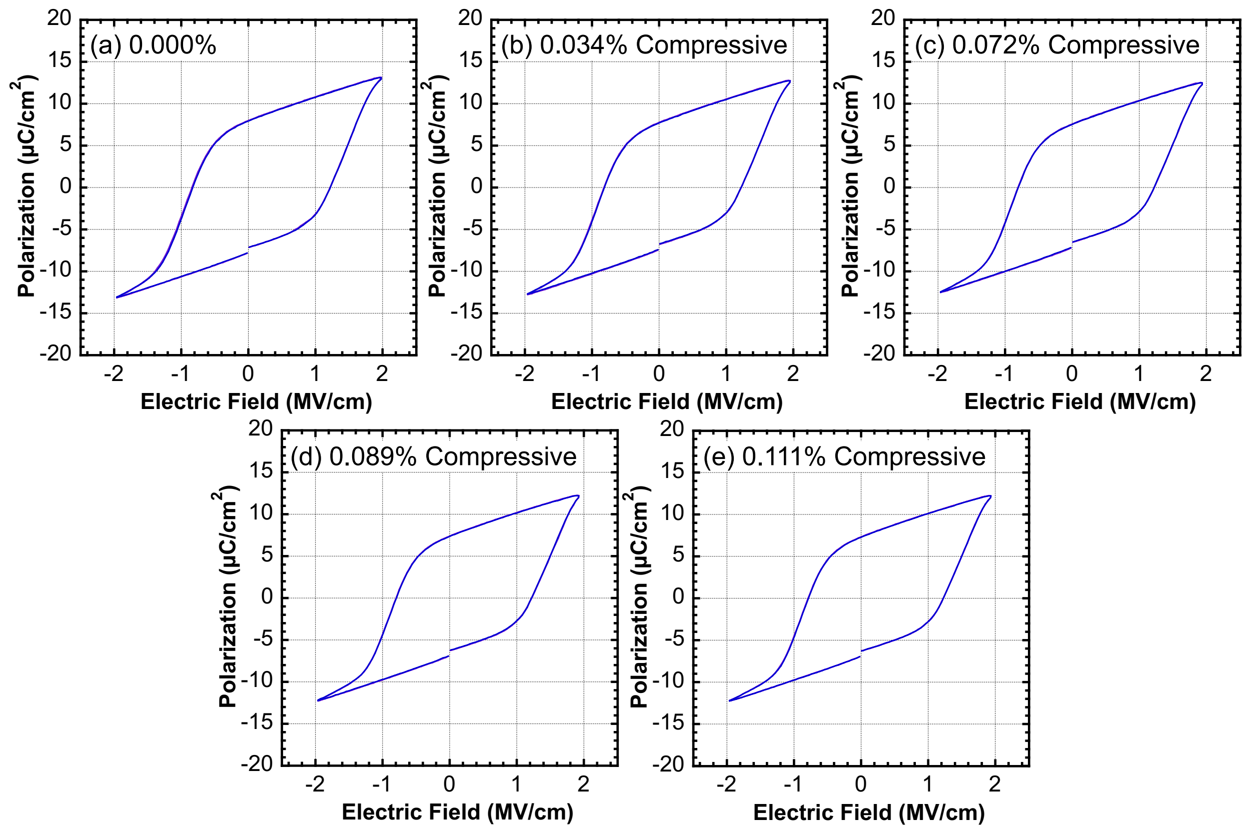

FIG. S3. Polarization versus electric field measured three different times for each in-plane strain state for TaN/HZO/TaN capacitors with extrinsic strains of (a) 0.000%, (b) -0.034%, (c) -0.072%, (d) -0.089%, and (e) -0.111%.